In memory of Professor Robert R. Gałązka

Effect of Non-Local Growth Dynamics on Magnetic Properties of Composition-Graded $Ga_{1-x}Mn_xAs_{1-y}P_y$ Ferromagnetic Films

S.-K. Bac[a,b], X. Liu[b], M. Dobrowolska[b], S. Lee[a] and J.K. Furdyna[b,*]

[a] *Department of Physics, Korea University, Seoul 02841, Republic of Korea*
[b] *Department of Physics, University of Notre Dame, Notre Dame, IN 46556, USA*

Doi: 10.12693/APhysPolA.141.149 *e-mail: furdyna@nd.edu

We discuss the magnetic properties of $Ga_{1-x}Mn_xAs_{1-y}P_y$ films with phosphorus content y graded along the growth direction from $y = 0.03$ to $y \approx 0.25$. Such grading was achieved by growing the film epitaxially in the form of sublayers with successively increasing values of y. X-ray measurements reveal that the strain in the film changes coherently with increasing phosphorus content, from in-plane compressive at the bottom to in-plane tensile in the upper sublayers of the graded film. The grading of strain arising from the changing composition results in gradual changes of magnetic anisotropy from in-plane in the lower sublayers to out-of-plane as we progress toward the top. Magnetization measurements reveal that the graded film is composed of three regions with different magnetic anisotropies: one with a strong in-plane easy axis, one with a strong out-of-plane easy axis, and in between a region with both in-plane and out-of-plane easy axes. The contribution of the region with an in-plane easy axis to the total magnetization of the film was found to be strongly dominant. This result is quite unexpected, because $\approx 75\%$ of the graded film consists of sublayers under tensile strain, where out-of-plane magnetic anisotropy is expected to dominate. These surprising results arise from effects occurring in epitaxial growth of such graded structures, where properties of a layer being deposited are determined not only by growth conditions at the moment of deposition but also by the presence of layers grown earlier and by deposition of additional layers grown later. This form of growth can be explained in terms of band structure at different locations of the multilayer as the growth proceeds, and we will therefore refer to it as non-local growth.

topics: ferromagnetic semiconductors, magnetic anisotropy, semiconductor alloys with graded composition, epitaxial growth dynamics

1. Introduction

GaAs-based ferromagnetic semiconductors (FMSs) such as $Ga_{1-x}Mn_xAs$ are receiving wide attention owing to their carrier-mediated ferromagnetism, which can be conveniently controlled by various external means, thus making these materials of interest as candidates for spintronic devices [1–3]. Their growth by low-temperature molecular beam epitaxy (LT-MBE) is now well established [4, 5], and their magnetic properties are known to depend on the following parameters: the concentration of substitutional and interstitial Mn, the concentration of holes, and strain [6–8]. Importantly, strain is known to play a decisive role in determining the magnetic anisotropy of these materials, establishing the orientation of easy axes of magnetization [9]. For example, GaAs-based FMS films under compressive strain prefer the magnetic easy axis to lie in the film plane, while films under tensile strain prefer an out-of-plane easy axis orientation [10, 11]. This characteristic feature is consistently observed in uniform single-layer FMS films, such as $Ga_{1-x}Mn_xAs$ and $Ga_{1-x}Mn_xAs_{1-y}P_y$ grown on various substrates [12–15].

In this paper, we have undertaken a study of the magnetic properties of FMS film, in which the strain is systematically graded along the film thickness. We approached this by growing a multilayer of the quaternary ferromagnetic semiconductor $Ga_{1-x}Mn_xAs_{1-y}P_y$ in which the concentration of phosphorus is increased in successively deposited sublayers. Since the tetrahedral radius of P is significantly smaller than that of As [16], the substitution of P at the As sites will increase the degree of tensile strain in such a system, as the concentration of P is increased.

However, the gradient of P concentration in this structure leads not only to a gradient of strain but also to a gradient of the semiconductor band structure along the film thickness [17]. As will be

shown, such grading of the band structure during the growth will then also lead to a novel character of epitaxial growth, in which the properties of a specific epitaxial sublayer of the graded system will depend not only on the growth conditions used during the deposition of the sublayer, but also on the properties of sublayers deposited before and later. Because in this growth process the formation of the sample at one location depends on the properties of the samples in other locations, we will refer to it as non-local growth. As will be shown, this has significant — and quite unexpected — consequences in the resulting magnetic properties of the graded GaAs-based FMSs, such as those observed in the graded $Ga_{1-x}Mn_xAs_{1-y}P_y$ system studied here.

2. Experiments

The graded $Ga_{1-x}Mn_xAs_{1-y}P_y$ sample was grown on a GaAs (001) substrate in a Riber 32 molecular beam epitaxy (MBE) system. Grading of phosphorus concentration along the growth direction was achieved by growing eight thin sublayers with successively increasing phosphorus concentration y, which was controlled by a mechanical valve equipped with a rapid flux control mechanism. The growth temperature of the FMS layers was kept at 260°C. As each successive sublayer of the structure was deposited, the P_2/As_2 flux ratio was systematically increased, while the As_2/(Ga, Mn) flux ratio was kept unchanged during the entire growth. This process resulted in a graded ≈ 100 nm $Ga_{1-x}Mn_xAs_{1-y}P_y$ multilayer, consisting of eight sublayers of ≈ 12.5 nm in which y varied from 0.03 to 0.24 in steps Δy of ≈ 0.03. During the entire growth process, the Mn concentration x was kept constant at $x \approx 0.06$.

2.1. Structural characterization

The structure of the graded $Ga_{1-x}Mn_xAs_{1-y}P_y$ film obtained in this manner is schematically shown in Fig. 1a. In Fig. 1b we show the results of energy dispersive X-ray (EDX) measurements obtained by Dong et al. [18] on a very similar multilayer, grown in an identical manner, showing the distribution of arsenic and phosphorus concentration along the growth direction in such a graded multilayer. Crystallographic properties of the specimen were examined by high-resolution X-ray diffraction (HR-XRD) using a Bruker D8 Discover X-ray diffractometer, as described in [18].

HR-XRD measurements confirm the overall crystal integrity of the graded sample. Figure 2 shows reciprocal space mapping of the sample at the $(\bar{2}\bar{2}4)$ diffraction peak. Q_z and Q_x correspond to the inverse of vertical and lateral lattice constants of the crystal, respectively. The fact that all peaks occur at the same Q_x position in Fig. 2 confirms that the lattice of the graded $Ga_{0.94}Mn_{0.06}As_{1-y}P_y$ film is fully strained by the GaAs substrate, i.e,

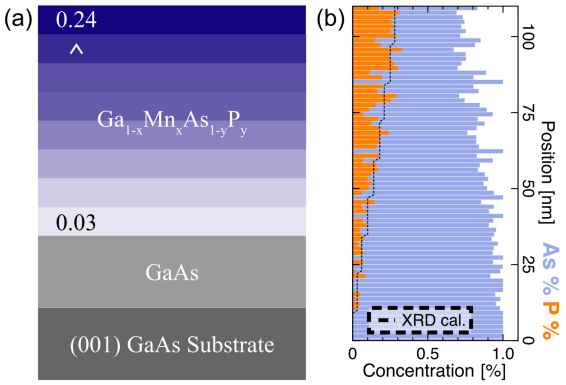

Fig. 1. (a) Schematic of graded $Ga_{1-x}Mn_xAs_{1-y}P_y$ film, consisting of eight sublayers with successively increasing concentration of P. (b) EDX results obtained earlier by our team on a similar multilayer [18], showing concentrations of P and As along the growth direction.

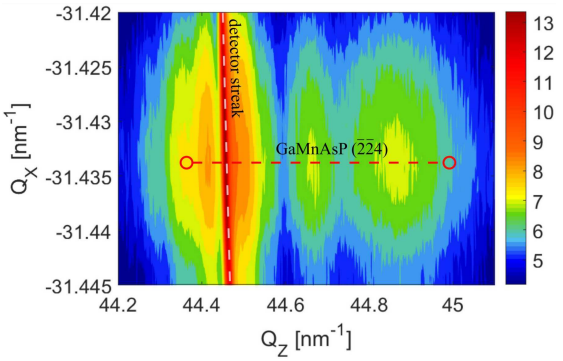

Fig. 2. Reciprocal space map in the vicinity of the $(\bar{2}\bar{2}4)$ Bragg reflection of the graded film.

that the in-plane lattice parameter remains unchanged throughout the entire sample thickness, even though the P concentration is varied from $y \approx 0.03$ up to $y \approx 0.24$.

Figure 3a shows a 2θ–ω diffraction scan measured along the growth direction (which in this paper will be referred to as the c-direction) of the graded film.

- The sharpest peaks located at $\approx 66°$ represents the (004) Bragg reflection of the GaAs substrate;
- The series of weaker maxima marked by black arrows are the Bragg peaks corresponding to $Ga_{0.94}Mn_{0.06}As_{1-y}P_y$ sublayers deposited with successively increasing values of y;
- The lower-intensity oscillations are Pendellosung fringes, attesting to the uniform thickness of the multilayer.

The positions of the maxima marked by arrows were identified by comparing the XRD spectrum in Fig. 3a to EDX measurements similar to those

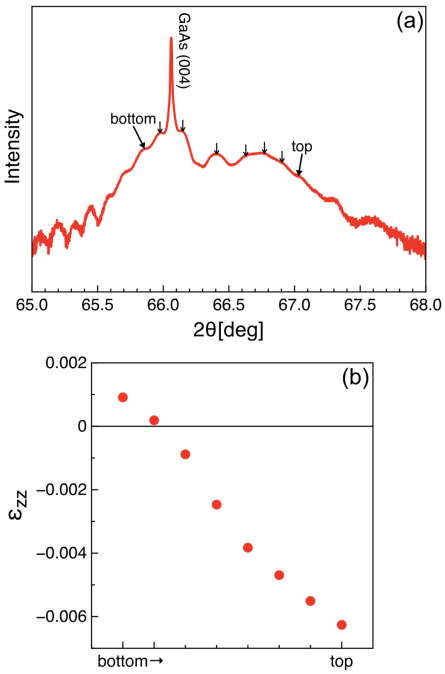

Fig. 3. (a) HR-XRD 2θ–ω spectrum of graded $Ga_{1-x}Mn_xAs_{1-y}P_y$ film. (b) Progression of strain ε_{zz} for the eight sublayers of the graded film, from bottom to top.

shown in Fig. 1b, which indicate the quantitative changes of the P concentration along the c direction. The X-ray data clearly shows the progressive reduction of the lattice constant along the c-direction, in line with increasing in-plane tensile strain in successive $Ga_{0.94}Mn_{0.06}As_{1-y}P_y$ sublayers.

To quantitatively determine the strain in each sublayer of the graded film, we use the equation for out-of-plane strain ε_{zz} given by

$$\varepsilon_{zz} = \frac{c - a_0}{a_0}, \qquad (1)$$

where a_0 is the relaxed lattice constant for the sublayer with a given y, and c is the lattice spacing along the c-direction measured by HR-XRD. The values of ε_{zz} for the eight sublayers are plotted in Fig. 3b. The bottom two $Ga_{0.94}Mn_{0.06}As_{1-y}P_y$ sublayers show positive values of ε_{zz}, thus indicating compressive in-plane strain, while the remaining six sublayers show negative values of ε_{zz}, indicating tensile strain. Note that the magnitude of the strain changes monotonically from compressive to tensile from the bottom of the multilayer to the top, consistent with the systematically increasing concentration of phosphorus in the sample. One would then expect that the magnetization of the bottom two sublayers would be characterized by in-plane easy axes, while the easy axes in the remaining six sublayers (amounting to $\approx 75\%$ of the sample's volume, and thus to its total magnetization, since the concentration of Mn is the same along the sample thickness) would be out-of-plane.

2.2. Magnetic properties of the graded film

To investigate the magnetic properties of our graded $Ga_{0.94}Mn_{0.06}As_{1-y}P_y$ film, the magnetization of the film was measured by a superconducting quantum interference device (SQUID). The temperature dependences of magnetization measured with a 25 G field applied along the [010] (in-plane) and the [001] (out-of-plane) directions are shown in Fig. 4a. Surprisingly, the data show that, contrary to expectation, the value of the in-plane magnetization of the sample is larger than its out-of-plane magnetization at all temperatures below the Curie temperature. This preference for the in-plane magnetization of the graded film is also evident in the hysteresis loops measured at 5 K with magnetic field along the [010] and [001] directions shown in Fig. 4b, with the remanent magnetization at zero field also significantly larger for the in-plane results.

Interestingly, the out-of-plane magnetization hysteresis shows a strikingly complex behavior, indicating that the reversal of the out-of-plane magnetization in the graded sample involves a sequence of steps. We show that such multiple transitions observed during magnetization reversal can be explained by assuming that the graded sample consists of three regions with different magnetic anisotropies: one with an out-of-plane easy axis, one with an in-plane easy axis, and an intermediate region with both in-plane and out-of-plane easy axes, as suggested schematically by thick arrows at the top of Fig. 5b. We note parenthetically that these three regions may each consist of several sublayers with different values of y, and the boundaries between these regions need not coincide with boundaries between compositional sublayers. The formation of such regions and their extents is expected to arise from the interplay of magnetizations with different anisotropies as they form successively in the graded film. A similar behavior, including the spontaneous formation of an intermediate region,

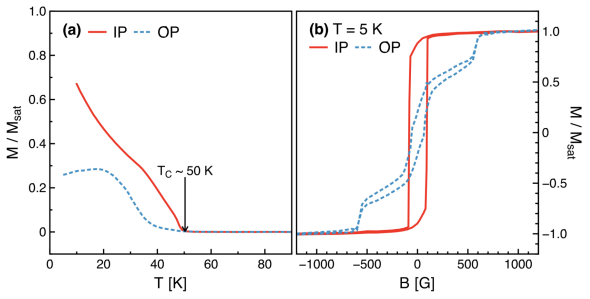

Fig. 4. (a) Temperature dependence of magnetization of the $Ga_{0.94}Mn_{0.06}As_{1-y}P_y$ graded film, measured with a field of 25 G applied in the [010] (red solid line) and [001] (blue dotted line) directions. (b) Hysteresis loops of the graded sample measured at 5 K with the magnetic field swept along the [010] (red solid line) and [001] (blue dotted line).

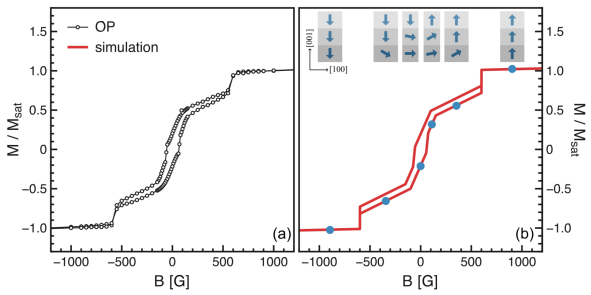

Fig. 5. (a) Hysteresis loops of the $Ga_{0.94}Mn_{0.06}As_{1-y}P_y$ graded film measured at 5 K with the magnetic field applied along the [001] (out-of-plane) direction. (b) Simulation of combined contributions of the three regions magnetic with different anisotropies. The insets at the top indicate magnetization alignments in the three regions at positions marked with solid circles.

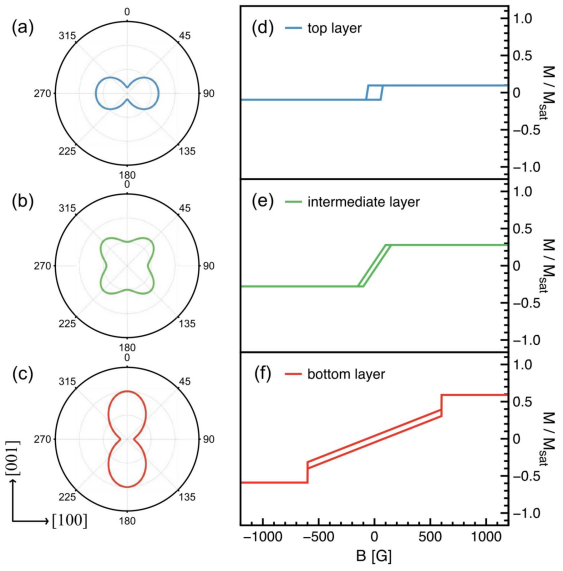

Fig. 6. (a)–(c) Projections of magnetic free energy diagram on the (010) plane for the three magnetic regions of the graded sample. (d)–(f) Expected magnetization hystereses for the three magnetic anisotropies during an out-of-plane field scan, plotted separately. Magnitudes are obtained from simulation in Fig. 5b.

has also been observed in GaMnAs/GaMnAsP bilayers in which in-plane and out-of-plane magnetic anisotropies interface with one another [19, 20].

Projections of magnetic free energy on the (010) plane for the three regions with different magnetic anisotropies are shown in Fig. 6a–c. In the bottom region, represented by Fig. 6c, the easy axis is in-plane, pointing along 90° or 270°. In the top region (Fig. 6a) it is out-of-plane, pointing along 0° or 180°. In turn, in the intermediate (transition) layer (Fig. 6b) there are two easy axes, one in-plane, along 90° or 270°, and one out-of-plane, along 0° or 180°. We can now simulate the total magnetization reversal of the graded film shown in Fig. 5a, by adjusting the magnitudes of each region's contribution and superimposing them. The magnitudes that give the best fit to the data in Fig. 5 are shown on the y-axis in Fig. 5d–f, indicating the expected contributions of each region to the out-of-plane field scan.

This approach then allows us to estimate the fraction of the total magnetization of the film contributed by each of the three regions: the region with an out-of-plane easy axis accounts for $\approx 12.5\%$ of the total magnetization, the region with in-plane easy axes contributes $\approx 62.5\%$, and the fraction with both in-plane and out-of-plane easy axes accounts for $\approx 25\%$. The coexistence of such three regions with different magnetic anisotropies in a graded $Ga_{1-x}Mn_xAs_{1-y}P_y$ film was also observed in an earlier investigation, in which anomalous Hall effect measurements were analyzed to obtain the portion of the film characterized by the three types of magnetic anisotropy [21].

Based on the division of the graded film into three regions with different magnetic behaviors, the multi-step magnetization reversal can be visualized as indicated by the thick arrow at the top of Fig. 5b. It shows the orientations of magnetization in the three regions at positions marked with solid circles in the hysteresis curve in Fig. 5b. Qualitatively, the presence of distinct regions with different anisotropies in the graded $Ga_{1-x}Mn_xAs_{1-y}P_y$ film is reasonable if one considers the change of strain from compressive to tensile along the thickness of the film [15]. However, the relative contributions of the different magnetic anisotropies to the total magnetization of the sample, particularly the dominance of in-plane anisotropy, is at first glance completely unexpected. As shown in Fig. 1d, the portion of the film under tensile strain, which is expected to exhibit magnetization with an out-of-plane easy axis, corresponds to about 75% of the sample, but the observed fraction of magnetization with such orientation is only about 12.5%. On the other hand, the measured fraction of magnetization with in-plane anisotropy amounts to 62.5% of the graded film, although only two of the eight sublayers are under compressive strain, as shown in Fig. 3b. Such an unexpectedly large discrepancy between strain conditions in the graded film and its magnetic properties implies the presence of some additional mechanism that has not been considered.

3. Non-local growth dynamics of graded ferromagnetic semiconductor films

An important mechanism to consider in the present context is the process of low-temperature MBE growth specific to a GaAs-based ferromagnetic semiconductor such as $Ga_{1-x}Mn_xAs$ or $Ga_{1-x}Mn_xAs_{1-y}P_y$, and how the incorporation of magnetic ions (in the present case of Mn) takes place during the growth of a graded structure.

We recall that the incorporation of Mn into the $Ga_{1-x}Mn_xAs_{1-y}P_y$-based FMS lattice occurs in three forms: primarily at substitutional positions, where Mn replaces Ga and becomes an acceptor; to a lesser extent at interstitial positions, where Mn ions become double donors; and also in the form of neutral Mn precipitates [7, 22]. The effect of Mn precipitates on magnetic properties was shown to be minimal [23, 24], and we will ignore them in this discussion.

We will designate the concentration of substitutional and interstitial Mn by $x_{\rm sub}$ and $x_{\rm i}$, respectively. As noted, the substitutional Mn is an acceptor and thus also produces $x_{\rm sub}$ holes, which provide the mechanism of magnetic exchange between magnetic moments of Mn in the FMS system, and are thus essential for its ferromagnetism. Mn interstitials, on the other hand, are double donors, thus compensating for the holes produced by the substitutional Mn. Additionally, since Mn interstitials are mobile and positively charged, they drift toward the fixed positions of the negatively-charged substitutional Mn, forming antiferromagnetically-aligned Mn–Mn pairs and canceling the magnetic moments of the substitutional Mn in those pairs. We can now express the concentrations of *net* magnetic moments in the crystal (i.e, those that determine the value of magnetization) as $x_{\rm eff} = x_{\rm sub} - x_{\rm i}$, and the number of active holes as $x_p = x_{\rm sub} - 2x_{\rm i}$.

To discuss the distribution of Mn during the growth of $Ga_{1-x}Mn_xAs_{1-y}P_y$ with a graded value of y, we must also consider the band structure of the graded film. Figure 7 shows how the top of the valence band is expected to progress with increasing phosphorus concentration in the eight sublayers of our graded $Ga_{0.94}Mn_{0.06}As_{1-y}P_y$ film. We will assume that at the growth temperature (260°C) the acceptors are ionized, and are in the valence band. Since the top of the valence band of GaP lies $\approx$ 400 meV lower than that of $Ga_{1-x}Mn_xAs$ [25] and the phosphorus concentration is increased by about 3% in each successive sublayer, the top of the valence band will move progressively *downward* by about 10 meV in each sublayer, as indicated schematically in Fig. 7. We will show that this staircase-like valence band profile will lead to interesting non-local growth dynamics of the graded multilayer, and will result in important modifications of its magnetic properties.

It is well established that in $Ga_{1-x}Mn_xAs$-based FMS systems the incorporation of substitutional Mn at Ga sites is limited by the Fermi energy, as discussed by Yu et al. [23] and that this leads to the formation of Mn interstitials when the concentration of holes due to $x_{\rm sub}$ exceeds a certain limit. This feature will have a major impact on the growth of our graded multilayer structure, and it is instructive to discuss this process sublayer-by-sublayer. The first ($y = 0.03$) sublayer of the graded $Ga_{0.94}Mn_{0.06}As_{1-y}P_y$ film will grow according to the local MBE growth conditions determined by

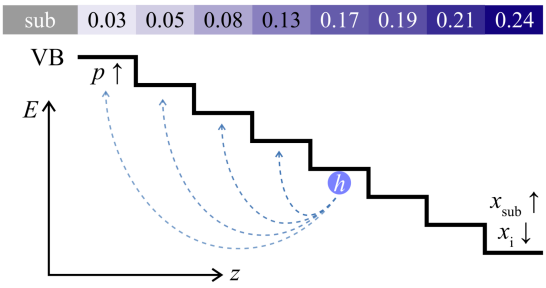

Fig. 7. Schematic diagram of our graded film. The bar at the top shows the progression of phosphorus concentrations, indicated by shading. The main figure shows the top of the valence band for the eight sublayers of the $Ga_{0.94}Mn_{0.06}As_{1-y}P_y$ film, each step corresponding to a drop of $\approx$ 10 meV. Dashed arrows indicate hole drainage from sublayers with larger y to those with lower y as the growth proceeds.

growth temperature and elemental fluxes, and will result in the values of $x_{\rm sub}$ and $x_{\rm i}$ that correspond to those conditions. However, when the 2nd sublayer ($y = 0.05$ in Fig. 7) is deposited on sublayer 1, the band offset between the two layers will become important. As shown by Wojtowicz et al. [26] in their modulation-doping experiments, some of the holes forming in layer 2 will be siphoned off into sublayer 1 due to the band offset between these sublayers, as indicated by the dashed arrows in Fig. 7. That will automatically lower the Fermi energy in sublayer 2, thus allowing $x_{\rm sub}$ to increase, and significantly reduce the concentration of $x_{\rm i}$ forming in this layer. As a consequence, both sublayers will end up with different magnetic properties than they would if they were grown separately.

The concentration of holes in sublayer 1 will now be greater, resulting in higher magnetization [27]. The number of active magnetic ions in sublayer 2 will be higher. Although some of the holes in sublayer 2 will be siphoned off to sublayer 1, they will be replenished by a similar process when sublayer 3 is grown. As a consequence, the magnetization of both layers will be higher than if they were grown separately.

Similarly, as sublayer 3 is being grown, the holes produced by substitutional incorporation of Mn will be siphoned off to the preceding sublayer(s), again allowing a higher substitutional and lower interstitial incorporation of Mn than would be the case if the layer were grown separately, as an independent film. We can now make the same argument for sublayers 4, 5, etc. Namely, as each successive sublayer is grown, the holes will be drained off to sublayer(s) grown earlier, allowing the sublayer being grown to end up with a larger substitutional incorporation of Mn at Ga sites, and consequently a lower concentration of the harmful mobile interstitials. Moreover, although the concentration of holes in each sublayer is reduced by migration to layers grown earlier,

it is replenished by holes from sublayers grown later. Consequently, the final properties of each sublayer depend not only on the local growth conditions that existed at the moment of its deposition, but on what had occurred at other locations of the multilayer.

While this non-local process would appear to lead to increased magnetization in all sublayers owing to higher substitutional incorporation of Mn, there are important trade-offs that must be considered. As each new sublayer is grown, the holes themselves — of key importance for the ferromagnetism of the system — are drained off to sublayers grown earlier, as argued above, resulting in a significant hole deficit in the uppermost sublayers of the film. While we are not able to discuss this process quantitatively, it is likely that, as the number of sublayers already grown increases, their effectiveness of draining holes from sublayers grown later will also increase, by analogy with modulation doping experiments of Wojtowicz et al., where it was shown that the effectiveness of a doped barrier in modulation doping is proportional to its thickness [26]. On the other hand, the degree of such hole drainage will of course be limited by the Coulomb attraction between the migrating holes and the negative charge of parent acceptor centers which the holes left behind. At this stage, we are not able to discuss this process quantitatively, but it appears reasonable that the drainage of holes to the sample region which was grown earlier will result in the dominance of that region in determining the overall magnetic properties of the graded multilayer structure.

The process described above naturally occurs at the growth temperature, in the present case of about 260°C, at which the holes are ionized and free to move in the valence band. On the other hand, to discuss the ferromagnetic behavior of the graded specimen, we must consider its properties at temperatures below its Curie temperature, as shown in Figs. 4 and 5, where the holes are expected to reside in the impurity band. It is therefore important to note that the concentrations of substitutional and interstitial Mn ions, which are established during the growth, as determined by the migration of holes at the growth temperature, are fixed, becoming the structural property of the specimen. Establishing the distribution of holes when the specimen is cooled will, however, be modified by the Coulomb fields created at the sublayer boundaries by hole migration, which require further analysis.

The growth dynamics of a graded film described above explain quite nicely the dominance of its in-plane magnetization. As new sublayers are deposited, the concentration of holes in sublayers already grown (i.e, those favoring in-plane anisotropy) grows both by hole drainage from layers grown later, and (except for sublayer 1) by the lower rate of formation of Mn interstitials. This growth process results in a disproportional increase of magnetization in the lower layers, consistent with the observed magnetization anisotropy.

4. Conclusions

We have shown that when a graded ferromagnetic semiconductor film is grown, the final properties of any section of the film are determined not only by the conditions that existed at the time of its growth, but by what had already been grown and — surprisingly — by what was grown later. This is particularly true when the magnetic properties of the material at any location depend on the concentration of mobile charge carriers, and when the grading of composition also involves grading of the valence band offset, as is the case of the quaternary ferromagnetic semiconductor $Ga_{0.94}Mn_{0.06}As_{1-y}P_y$ investigated in this paper. In that case, the concentrations of Mn incorporated substitutionally at Ga sites and interstitially in a given sublayer are determined not only by the growth conditions that exist when that sublayer is deposited, but by what layers had been grown before. This will then have profound consequences on how this sublayer contributes to the overall magnetic properties of the graded system.

The redistribution of charges during such non-local growth involves two mechanisms: the tendency of the holes to seek lower energy by migrating to regions where the top of the valence band is higher, and the Coulomb attraction between the migrating holes and their negatively-charged parent acceptor centers, which the holes leave behind as they migrate. It is a simple matter to describe this process qualitatively, as has been done in this paper. To obtain a quantitative picture of non-local growth, however, one will need to relate the value of the band offset at the time and location where growth occurs to the distribution of substitutional and interstitial Mn ions, to the resulting formation of uncompensated free carriers, and to the Coulomb field produced by their migration. Analysis of this type is outside the scope of the present paper.

Acknowledgments

This research was supported by Basic Science Research Program through the National Research Foundation of Korea (NRF) of Korea (2021R1A2C1003338); by the NRF under the BK21 FOUR program at Korea University, Initiative for Science Frontiers on Upcoming Challenges; by Korea University Grant; and by National Science Foundation Grant DMR 1905277.

References

[1] A.H. MacDonald, P. Schiffer, N. Samarth, *Nature Mater.* **4**, 195 (2005).

[2] T. Dietl, H. Ohno, *Rev. Mod. Phys.* **86**, 187 (2014).

[3] T. Dietl, A. Bonanni, H. Ohno, *J. Semicond.* **40**, 080301 (2019).

[4] T. Hayashi, M. Tanaka, T. Nishinaga, H. Shimada, H. Tsuchiya, Y. Otuka, *J. Cryst. Growth* **175**, 1063 (1997).

[5] A. Shen, F. Matsukura, S.P. Guo, Y. Sugawara, H. Ohno, M. Tani, H. Abe, H.C. Liu, *J. Cryst. Growth* **201**, 679 (1999).

[6] T. Dietl, H. Ohno, F. Matsukura, *Phys. Rev. B* **63**, 195205 (2001).

[7] K.M. Yu, W. Walukiewicz, T. Wojtowicz, I. Kuryliszyn, X. Liu, Y. Sasaki, J.K. Furdyna, *Phys. Rev. B* **65**, 201303 (2002).

[8] T. Jungwirth, J. Sinova, J. Mašek, J. Kučera, A.H. MacDonald, *Rev. Mod. Phys.* **78**, 809 (2006).

[9] X. Liu, Y. Sasaki, J.K. Furdyna, *Phys. Rev. B* **67**, 205204 (2003).

[10] K. Hamaya, T. Taniyama, Y. Kitamoto, T. Fujii, Y. Yamazaki, *Phys. Rev. Lett.* **94**, 147203 (2005).

[11] L. Thevenard, L. Largeau, O. Mauguin, G. Patriarche, A. Lemaître, N. Vernier, J. Ferré, *Phys. Rev. B* **73**, 195331 (2006).

[12] J. Zemen, J. Kučera, K. Olejník, T. Jungwirth, *Phys. Rev. B* **80**, 155203 (2009).

[13] M. Glunk, J. Daeubler, L. Dreher et al., *Phys. Rev. B* **79**, 195206 (2009).

[14] A. Lemaître, A. Miard, L. Travers, O. Mauguin, L. Largeau, C. Gourdon, V. Jeudy, M. Tran, J.M. George, *Appl. Phys. Lett.* **93**, 021123 (2008).

[15] X. Li, X. Liu, S. Dong, C. Gorsak, J.K. Furdyna, M. Dobrowolska, S.-K. Bac, S. Lee, S. Rouvimov, *J. Vac. Sci. Technol. B* **36**, 02D104 (2018).

[16] J.A. Van Vechten, J.C. Phillips, *Phys. Rev. B* **2**, 2160 (1970).

[17] T.J. Grassman, M.R. Brenner, M. Gonzalez, A.M. Carlin, R.R. Unocic, R.R. Dehoff, M.J. Mills, S.A. Ringel, *IEEE Trans. Electron Dev.* **57**, 3361 (2010).

[18] Sining Dong, Yong-Lei Wang, Seul-Ki Bac et al., *Phys. Rev. Mater.* **3**, 074407 (2019).

[19] Xiang Li, Seul-Ki Bac, Sining Dong, Xinyu Liu, Sanghoon Lee, S. Rouvimov, M. Dobrowolska, J.K. Furdyna, *AIP Adv.* **8**, 056401 (2018).

[20] Suho Choi, Seul-Ki Bac, Xinyu Liu, Sanghoon Lee, Sining Dong, M. Dobrowolska, J.K. Furdyna, *Sci. Rep.* **9**, 1 (2019).

[21] Seul-Ki Bac, Sanghoon Lee, Xinyu Liu, M. Dobrowolska, B.A. Assaf, J.K. Furdyna, *Phys. Rev. Mater.* **5**, 054414 (2021).

[22] T. Wojtowicz, J.K. Furdyna, X. Liu, K.M. Yu, W. Walukiewicz, *Physica E* **25**, 171 (2004).

[23] K.M. Yu, W. Walukiewicz, T. Wojtowicz, W.L. Lim, X. Liu, U. Bindley, M. Dobrowolska, J.K. Furdyna, *Phys. Rev. B* **68**, 041308(R) (2003).

[24] T. Wojtowicz, W.L. Lim, X. Liu, Y. Sasaki, U. Bindley, M. Dobrowolska, J.K. Furdyna, K.M. Yu, W. Walukiewicz, *J. Superconduct.* **16**, 41 (2003).

[25] I. Vurgaftman, J.R. Meyer, L.R. Ram-Mohan, *J. Appl. Phys.* **89**, 5815 (2001).

[26] T. Wojtowicz, W.L. Lim, X. Liu, M. Dobrowolska, J.K. Furdyna, K.M. Yu, W. Walukiewicz, I. Vurgaftman, J.R. Meyer, *Appl. Phys. Lett.* **83**, 4220 (2003).

[27] H. Ohno, A.D. Chiba, A.F. Matsukura, T. Omiya, E. Abe, T. Dietl, Y. Ohno, K. Ohtani, *Nature* **408**, 944 (2000).